

Inhibition of autophagy enhances cinobufagin-induced apoptosis in gastric cancer

XUANXUAN XIONG^{1*}, BO LU^{1*}, QINGZHONG TIAN^{2*}, HAIYAN ZHANG¹, MINGBO WU¹,
HAO GUO², QIANJIN ZHANG², XIANGCHENG LI³, TIAN ZHOU¹ and YUN WANG^{2,3}

¹Department of Gastroenterology 2, Xuzhou City Central Hospital,
The Affiliated Hospital of the Southeast University Medical School (Xuzhou), Xuzhou, Jiangsu 221009;

²Department of Oncological Surgery, Xuzhou City Central Hospital,
The Affiliated Hospital of the Southeast University Medical School (Xuzhou),
The Tumor Research Institute of Southeast University (Xuzhou), Xuzhou, Jiangsu 221009;

³Key Laboratory of Living Donor Liver Transplantation, Ministry of Public Health,
Department of Liver Transplantation Center, The First Affiliated Hospital of
Nanjing Medical University, Nanjing, Jiangsu 210029, P.R. China

Received February 2, 2018; Accepted September 13, 2018

DOI: 10.3892/or.2018.6837

Abstract. Cinobufagin is a cardiotoxic bufanolide steroid secreted by the Asiatic toad *Bufo gargarizans*. Cinobufagin is one of the active ingredients in the anticancer Chinese medicine called Chan Su, which was demonstrated to be an effective treatment for gastric cancer. Increasing evidence shows that inhibition of autophagy has a pro-apoptotic effect on human gastric cancer cells. The aim of the present study was to investigate the relationship between cinobufagin, autophagy and apoptosis in gastric cancer. Autophagy was induced or inhibited in the human gastric cancer cell line SGC-7901 by incubation in HBSS media or by treatment with 3-methyladenine or *ATG5* siRNA, respectively. Following treatment, the levels of apoptosis, apoptotic proteins, reactive oxygen species (ROS), and mitochondrial membrane potential were compared between the conditions. As anticipated, we found that cinobufagin

increased apoptosis in SGC-7901 cells. Notably, inhibition of autophagy, monitored by the absence of the autophagosome marker LC3-II, also enhanced cell apoptosis. This effect was reversed when autophagy was induced by incubation in HBSS media. Enhanced expression of pro-apoptotic indicators, including BAX, cytosolic cytochrome *c*, cleaved PARP, caspase-3 and caspase-9, was detected when autophagy was suppressed. Increased pro-apoptotic protein expression was accompanied by disrupted mitochondrial membrane potential and elevated ROS production. Altogether, these data suggest that inhibition of autophagy enhances the anticancer action of cinobufagin through increased apoptosis of gastric cancer cells. Moreover, these effects may be partly mediated by ROS generation and the activation of the mitochondrial programmed cell death pathway.

Introduction

Gastric cancer is the fourth most frequently diagnosed cancer and the 2nd leading cause of cancer-related deaths worldwide (1). The morbidity and mortality rate of gastric cancer have decreased substantially over the past few decades, and attention has shifted to the key issue of prevention and treatment of gastric cancer. Increasing evidence implicates *Helicobacter pylori* in the development of gastric cancer. The initial bacterial infection leads to chronic gastritis and gastric ulcers, which may finally culminate in gastric cancer (2,3). The current treatments for gastric cancer include surgery, chemotherapy, radiotherapy, thermal therapy, immune therapy, and Chinese herbal treatment. However, due to the difficulty in diagnosing gastric cancer at an early stage, the prognosis with the current treatment options is often poor (4,5). Therefore, it is necessary to identify novel agents that more effectively treat advanced gastric cancer.

Cinobufagin is a cardiotoxic bufanolide steroid secreted by the Asiatic toad *Bufo gargarizans*. Chan Su, a traditional

Correspondence to: Dr Yun Wang, Department of Oncological Surgery, Xuzhou City Central Hospital, The Affiliated Hospital of the Southeast University Medical School (Xuzhou), The Tumor Research Institute of Southeast University (Xuzhou), 199 Jiefang South Road, Xuzhou, Jiangsu 221009, P.R. China
E-mail: wymvp52xx@gmail.com

Dr Tian Zhou, Department of Gastroenterology 2, Xuzhou City Central Hospital, The Affiliated Hospital of Southeast University Medical School (Xuzhou), 199 Jiefang South Road, Xuzhou, Jiangsu 221009, P.R. China
E-mail: 542193952@qq.com

*Contributed equally

Key words: gastric cancer, autophagy, cinobufagin, apoptosis, reactive oxygen species

Chinese medicine, is used to make a variety of valuable medicinal herbs. Bufalin, resibufogenin, and cinobufagin are the active ingredients in Chan Su. To date, several reports have detailed the antitumor effects of cinobufagin in gastric cancer (6-8). Additionally, research has demonstrated that cinobufagin may trigger apoptosis and autophagic cell death in gastric cancer via activation of the reactive oxygen species (ROS)/JNK/p38 axis. Interestingly, mutation of certain autophagy-related genes, such as ATG16L1 (autophagy related 16 like 1) and IRGM (immunity related GTPase M), confers susceptibility to gastric cancer (8). This suggests that there may be a close relationship between autophagy and the development of gastric cancer.

Autophagy is a pathophysiological process that enables the recycling of long-lived proteins or damaged organelles and is crucial for cell development, differentiation, survival and homeostasis (9-11). Many investigators have demonstrated the important role of autophagy in the development and progression of a wide range of cancers, including gastric cancer. It is believed that inhibition of autophagy in cancer cells could improve the toxicity of antitumor drugs and reverse drug resistance (12,13). In fact, we previously reported that knockdown of autophagy related 5 (*ATG5*) in hepatocellular carcinoma inhibits autophagy and enhances the antitumor effect of norcantharidin, a traditional Chinese medicine (14).

Previous studies have shown that cinobufagin and inhibition of autophagy both play anticancer roles in gastric cancer. Many reports have elucidated the cytotoxic effects of cinobufagin; however, little is known concerning the mechanism of cinobufagin-induced cytotoxic activity in gastric cancer (8,13). The mechanism of autophagy induction in gastric cancer and the connection between cinobufagin and autophagy are also not well established. Therefore, the objective of the present study was to elucidate the relationship of cinobufagin and autophagy in terms of their anticancer action.

Materials and methods

Reagents and materials. Cinobufagin was obtained from the National Institute for the Control of Pharmaceutical and Biological Products (Beijing, China). Cell Proliferation kit I (MTT) was purchased from Roche Applied Science (Mannheim, Germany). Hank's balanced salt solution (HBSS) was obtained from Sigma-Aldrich/Merck KGaA (Darmstadt, Germany). RPMI-1640 media, 10% heat-inactivated fetal bovine serum (FBS), and pancreatic enzymes were purchased from Gibco; Thermo Fisher Scientific, Inc. (Waltham, MA, USA). Antibodies, including β -actin (dilution 1:10,000; cat. no. ab227387), microtubule associated protein 1 light chain 3 (LC3-II) (dilution 1:3,000; cat. no. ab51520), caspase-3 (dilution 1:1,000; cat. no. ab2302), caspase-8 (dilution 1:1,000; cat. no. ab25901), caspase-9 (dilution 1:1,000; cat. no. ab32539), Bax (dilution 1:2,000; cat. no. ab32503), Bcl-2 (dilution 1:2,000; cat. no. ab182858) and cytochrome *c* (dilution 1:5,000; cat. no. ab133504) antibody were from Abcam (Cambridge, UK). Secondary antibody, included goat anti-rabbit IgG horseradish peroxidase (dilution 1:4,000; cat. no. ab6721) and goat anti-mouse IgG horseradish peroxidase (dilution 1:4,000; cat. no. ab205719) were from Abcam (Cambridge, UK).

Antibody against cleaved PARP was purchased from Santa Cruz Biotechnology, Inc. (dilution 1:500; cat. no. sc-56196; Santa Cruz, CA, USA). The mitochondrial membrane potential assay kit with JC-1 and RIPA lysis buffer was purchased from Beyotime Institute of Biotechnology (Suzhou, China). Enhanced chemiluminescence (ECL) detection kits and protease inhibitor were purchased from Pierce Biotechnology/Thermo Fisher Scientific, Inc. Horseradish peroxidase (HRP)-conjugated secondary antibody was obtained from Beijing Zhongshan Golden Bridge Biotechnology (Beijing, China).

Cell lines and treatment. The human gastric cancer cell line SGC-7901 was obtained from the Cell Bank of the Chinese Academy of Sciences (Shanghai, China). Cells were cultured in RPMI-1640 media supplemented with 10% fetal bovine serum, 50 U/ml penicillin, and 50 U/ml streptomycin and maintained in 5% CO₂ at 37°C.

Cells were divided into 8 groups: Sham, cinobufagin, HBSS, HBSC, 3-MA, 3-MAC, S and SC. To note, the HBSS, 3-MA and S groups were used as controls. The preliminary results showed no significant difference of the cell apoptotic ratio and LC3-II protein expression between the sham, HBSS, 3-MA and S groups. Therefore, for the simplicity of our results, the groups (sham, cinobufagin, HBSC, 3-MAC and SC) were used for all subsequent results of the experiments. i) Sham group: Cells were cultured in RPMI-1640 media. ii) Cinobufagin group: Cells were cultured in RPMI-1640 media containing cinobufagin (0, 0.03, 0.06, 0.12 or 0.24 mM) for 24 h (8). iii) HBSS group: Cells were cultured in HBSS media with Ca²⁺ and Mg²⁺ and supplemented with 10 mM HEPES (1 ml/well) for 0.5 h to induce autophagy (15). Following incubation in HBSS media, cells were washed twice with PBS and cultured in RPMI-1640 media for 24 h. iv) HBSC group: Cells were cultured in HBSS media as described for the HBSS group, and then cells were washed with PBS and cultured in RPMI-1640 media containing cinobufagin (0.24 mM) for 24 h. v) 3-MA group: Cells were cultured in RPMI-1640 media containing 3-MA (10 mM) (16). vi) 3-MAC group: Cells were cultured in RPMI-1640 media containing 3-MA (10 mM) to inhibit autophagy, washed twice with PBS, and cultured in RPMI-1640 media containing cinobufagin (0.24 mM) for 24 h. vii) S group: Cells were transfected with scrambled siRNA and cultured in RPMI-1640 media. viii) SC group (*ATG5* siRNA+cinobufagin): Cells were transfected with *ATG5* siRNA, cultured in RPMI-1640 media, washed twice with PBS, and then cultured in RPMI-1640 media containing cinobufagin (0.24 mM) for 24 h.

MTT assay. SGC-7901 cells were cultured in RPMI-1640 media on 96-well flat bottom microtiter plates at 1x10⁴ cells/well overnight, and treated with various concentrations of cinobufagin (0-0.5 mM) the following day. The cells were then incubated with MTT (20 μ l) solution (5 g/l) for 4 h at 37°C. An automatic multi-well spectrophotometer was used to calculate the absorbance value per well at 570 nm. All MTT assays were performed three times. The cell viability ratio was calculated with the following formula: Cell viability (%) = average absorbance of the treated group/average absorbance of the sham group x 100%. IC₅₀ values (50% inhibition concentration) were then calculated using the Statistical Package for the Social Sciences 17.0 (SPSS, Inc., Chicago, IL, USA).

RNA extraction and reverse transcription quantitative real-time PCR. Total RNA was isolated and purified from cells using TRIzol, and cDNA was synthesized with the PrimeScript RT Master Mix. Quantitative real-time PCR reactions were carried out using cDNA (2 μ l) as a template in a 20 μ l reaction. Primers were synthesized by Invitrogen; Thermo Fisher Scientific, Inc. (Shanghai, China). The primers utilized for RT-qPCR reactions were 5'-TTCTCAAATATACTGTTTC-3' (sense) and 5'-TATTATGTATCACAATGG-3' (antisense) for *ATG5*; 5'-TCACCCACACTGTGCCCATCTACGA-3' (sense) and 5'-CAGCGGAACCGCTCATTGCCAATGG-3' (antisense) for β -actin, and 5'-CCACTCTCCACCTTTGAC-3' (sense) and 5'-AGGGGAGATTCAGTGTGGTG-3' (antisense) for glyceraldehyde-3-phosphate dehydrogenase (*GADPH*). For RT-qPCR, the following cycles were used: 95°C for 30 sec, 40 cycles of 95°C for 5 sec, and 60°C for 31 sec. The dissociation stage used the following cycles: 95°C for 15 sec, 60°C for 1 min, and 95°C for 15 sec.

Small interfering RNA (siRNA) transfection. Small interfering RNAs (siRNAs) against *ATG5* and a nonspecific scrambled siRNA were purchased from Ambion (Austin, TX, USA). All siRNAs were synthesized by Qiagen (Chatsworth, CA, USA). SGC-7901 cells were cultured in 6-well plates. Invitrogen™ Lipofectamine 2000 (Thermo Fisher Scientific, Inc.) was mixed with RPMI-1640 media lacking 10% heat-inactivated FBS and containing siRNA1, siRNA2, or scrambled RNA. Mock controls were transfected with Lipofectamine 2000 alone. Transfections were performed at 37°C in 5% CO₂, after which the medium in each well was replaced by serum-containing medium for 4-6 h. After 2 h, cells were treated as indicated.

Western blot analysis. Total protein was extracted using Cell Lysis Reagents (Pierce) and quantified using the BCA method (Pierce; Thermo Fisher Scientific, Inc.). For cytochrome *c* analysis, cell pellets were suspended in HEPES buffer containing 250 mM sucrose and homogenized. The homogenate was then centrifuged at 800 x g and 4°C for 15 min. The supernatant was centrifuged at 10,000 x g for 15 min at 4°C. Mitochondrial pellets and cytosolic fractions were then collected (17). Proteins were separated on a 10% SDS-polyacrylamide gel and transferred to a PVDF membrane. The membrane was blocked and incubated with the primary antibodies overnight on a shaker in a cold room. Secondary antibodies (1:4,000) were applied for 1 h before visualization with an ECL detection kit. The gray value of each protein was measured by Image-Pro Plus 6.0 (National Institutes of Health, Bethesda, MD, USA) for statistical analyses.

Immunofluorescence. SGC-7901 cells were fixed on coverslips in 4% paraformaldehyde for 20 min. Afterwards, cells were blocked in 10% BSA for 1 h. Primary antibody (LC3-II in 10% BSA, 1:3,000; cat. no. ab51520; Abcam) was added overnight, followed by incubation with secondary antibody (1:1,000; cat. no. ab6721; Abcam) for 1 h at 37°C. Cells were then incubated with 4',6-diamidino-2-phenylindole (DAPI). Ten visual fields were chosen randomly, optical density was measured, and semi-quantitative analysis was performed with Image-Pro Plus 6.0.

Analysis of ROS production. Intracellular ROS levels were detected by flow cytometry using the dichlorodihydrofluorescein diacetate (DCHF-DA) assay. SGC-7901 cells were washed with D-Hank's solution three times, and then cells were cultured in RPMI-1640 media lacking FBS and containing DCHF-DA (100 μ M) at 37°C in the dark for 30 min. Afterwards, cells were washed with RPMI-1640 media lacking FBS and treated with pancreatic enzymes. DCF fluorescence was detected at an excitation wavelength of 488 nm and at an emission wavelength of 525 nm.

Annexin V and propidium iodide (PI) co-staining assay. Apoptosis was detected using the Annexin V-FITC kit. SGC-7901 cells were washed twice with ice-cold PBS and then resuspended in 400 μ l of binding buffer at a concentration of 5x10⁵ cells/ml. Next, 5 μ l of Annexin V-FITC and 5 μ l of PI were added to the cells. Tubes were gently vortexed and incubated for 15 min in the dark at 4°C. Samples were analyzed with a FACSCalibur flow cytometer (BD Biosciences, San Jose, CA, USA) using CellQuest software (BD Biosciences).

Mitochondrial membrane potential assay. Mitochondrial membrane potential was monitored by JC-1. The JC-1 dyeing liquid was added to each well (1 ml/well), and SGC-7901 cells were incubated at 37°C for 20 min. Afterwards, cells were washed twice with dyeing buffer (1X) and cultured in RPMI-1640 media. Finally, cells were observed by fluorescence microscopy (AX10; Carl Zeiss, Hamburg, Germany).

Statistical analysis. Data are expressed as mean \pm standard deviation. The significance of the differences between groups was determined by ANOVA and Dunnet's test. Multiple comparisons between the groups were performed using the S-N-K method after ANOVA. SPSS 17.0 software (SPSS, Inc., Chicago, IL, USA) was used for all statistical analyses, and P<0.05 was considered statistically significant.

Results

Cinobufagin inhibits SGC-7901 cell proliferation and induces caspase-mediated apoptosis. The MTT assay demonstrated that cinobufagin inhibited the proliferation of the SGC-7901 cells in a dose- and time-dependent manner after treatment with 0-0.5 mM cinobufagin for 12, 24 or 48 h (Fig. 1A). At concentrations >0.03 mM, cinobufagin treatment significantly inhibited cell proliferation. The IC₅₀ value of cinobufagin treatment at 24 h was 0.24 mM. Thus, a range of concentrations (0, 0.03, 0.06, 0.12 and 0.24 mM) was applied, and the concentration of 0.24 mM was used for all subsequent experiments.

Cinobufagin induces apoptosis in SGC-7901 cells. Cell apoptosis was detected by co-staining cells with Annexin V and PI. We found that the apoptotic ratio of SGC-7901 cells increased with cinobufagin treatment. The basal apoptotic population of the sham group was 2.77 \pm 1.04%. After treatment with cinobufagin at concentrations of 0.03, 0.06, 0.12, or 0.24 mM for 24 h, the apoptotic rate increased to 5.99 \pm 1.52, 8.35 \pm 2.55, 12.59 \pm 2.25 and 22.91 \pm 4.56%, respectively (Fig. 1B and C).

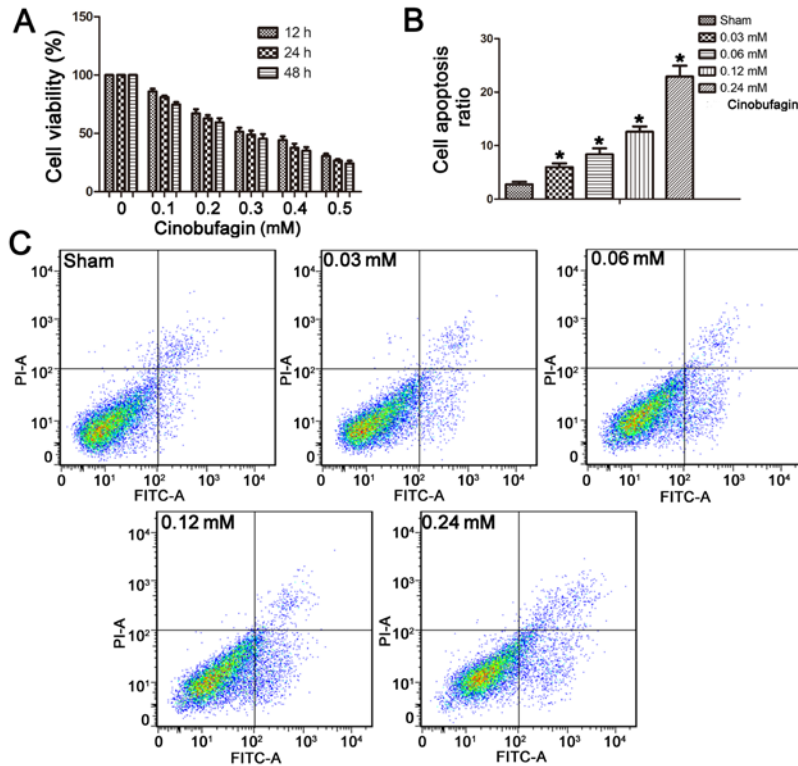


Figure 1. Cinobufagin induces apoptosis in SGC-7901 cells. (A) SGC-7901 cells were treated with 0-0.5 mM cinobufagin for 12, 24 or 48 h and proliferation was assessed with the MTT assay. (B and C) Cinobufagin pre-treated SGC-7901 cells were co-stained with Annexin V and PI to evaluate cell apoptosis ratios ($P < 0.05$ compared with the sham group). Both proliferation and apoptosis rate exhibited dose-dependent responses to cinobufagin treatment.

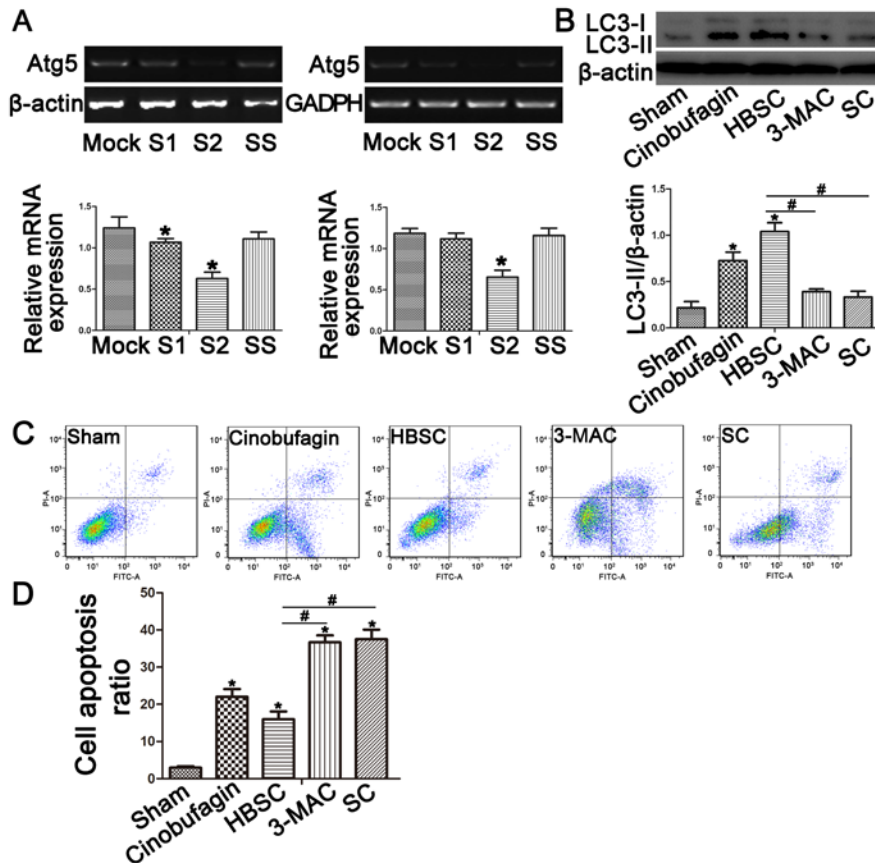


Figure 2. Inhibition of autophagy induces SGC-7901 cell apoptosis. (A) RT-qPCR analysis of ATG5 gene expression in the SC group compared with the Mock group ($P < 0.05$ compared with the Mock group). (B) HBSS-pretreatment increased LC3-II expression in the HBSC group, whereas LC3-II expression was inhibited by 3-MA or ATG5 siRNA in the SGC-7901 cells in the 3-MAC or the SC groups. (C and D) Annexin V and PI co-staining demonstrated that autophagy induction in the HBSC group decreased the early and late apoptosis rates compared with the sham group, whereas autophagy inhibition in the 3-MAC or the SC groups increased apoptosis rates of SGC-7901 cells ($P < 0.05$ compared with the sham group; $^{\#}P < 0.05$ compared with the HBSC group).

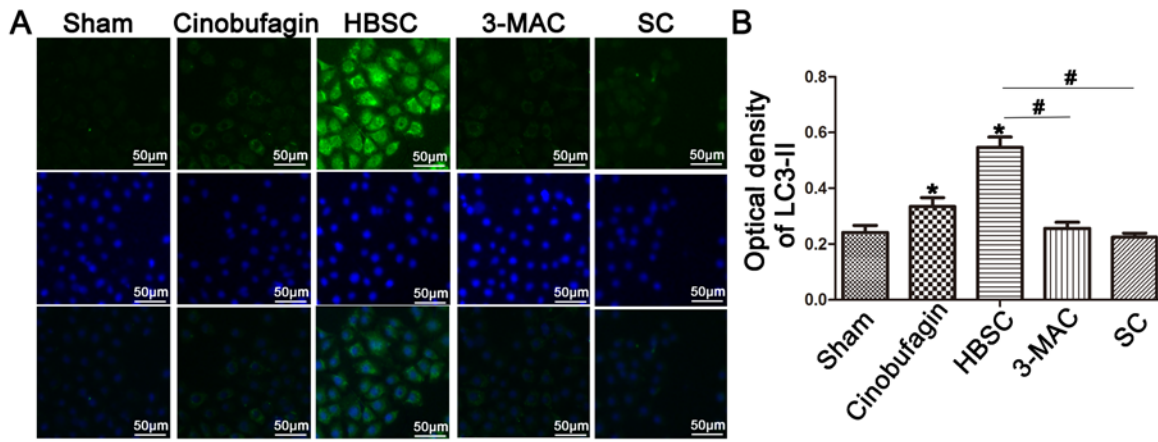


Figure 3. LC3-II immunofluorescence. (A and B) LC3-II staining was decreased in the 3-MAC and SC groups when observed by immunofluorescence, and photometric values of the protein were decreased as well. This effect was reversed in the HBSC group (*P<0.05 compared with the sham group; #P<0.05 compared with the HBSC group).

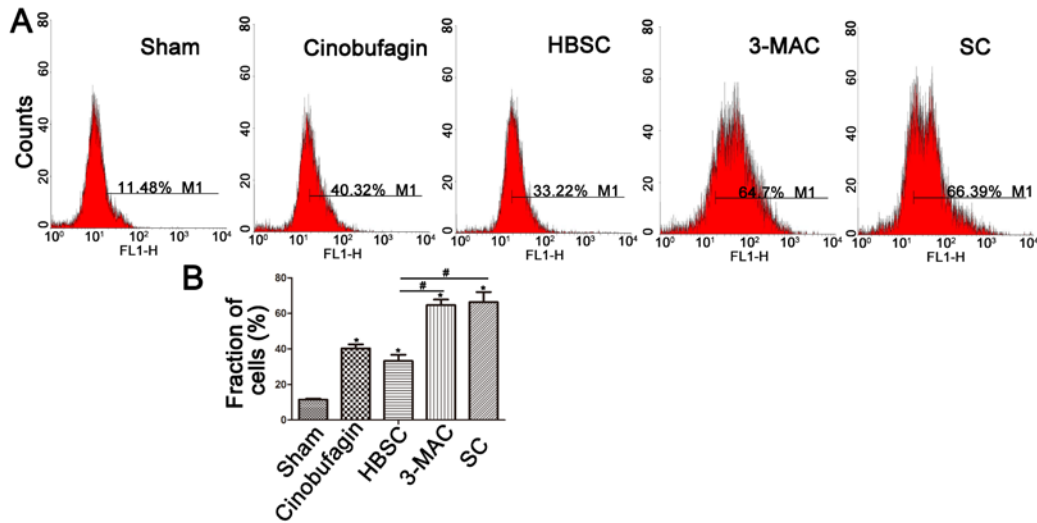


Figure 4. Relative oxygen species (ROS) generation is induced by cinobufagin and inhibition of autophagy. (A and B) Intracellular ROS generation was assessed by DCFH-DA assay and found to be increased in the cinobufagin group. Autophagy inhibition in the 3-MAC or the SC groups further enhanced the ROS generation compared with the cinobufagin group. However, when autophagy was induced in the HBSC group, ROS levels were downregulated (*P<0.05 compared with the sham group; #P<0.05 compared with the HBSC group).

This suggests a dose-dependent increase in apoptotic ratio in the SGC-7901 cells in response to cinobufagin treatment.

Autophagy counteracts cinobufagin-induced apoptosis.

To reduce autophagy activity, *ATG5* expression was knocked down by siRNA in SGC-7901 cells. RT-qPCR confirmed decreased *ATG5* gene expression in the SC group compared with the sham group (Fig. 2A; P<0.05). The autophagosome marker LC3-II was then used to monitor induction of autophagy by western blotting (Fig. 2B) and immunostaining (Fig. 3). When autophagy was inhibited by treatment with 3-MA or *ATG5* siRNA, LC3-II expression was reduced in the 3-MAC and SC groups compared with the sham group (Figs. 2B and 3; P<0.05). In contrast, western blotting and immunostaining revealed that SGC-7901 cells treated with HBSS displayed increased LC3-II protein levels (Figs. 2B and 3; P<0.05). To compare subsequent apoptosis ratios, SGC-7901 cells were co-stained with Annexin V and PI.

Staining demonstrated that inhibition of autophagy increased the apoptosis rates (Fig. 2C and D; P<0.05), whereas autophagy activation in the HBSC group reduced early and late apoptosis rates compared with the sham group (Fig. 2C and D; P<0.05).

ROS generation is induced by cinobufagin and is further enhanced by inhibition of autophagy.

ROS levels were then detected by DCFH-DA assay. Intracellular ROS generation was increased in the cinobufagin group and was further enhanced by inhibition of autophagy. However, ROS levels were downregulated when autophagy was induced (Fig. 4A and B).

Inhibition of autophagy induces Bax and cytochrome c, but reduces Bcl-2.

To further investigate the mechanism of cinobufagin-induced apoptosis, we detected the levels of apoptotic proteins by western blotting. As shown in Fig. 5, downregulation of autophagy increased Bax (Bcl-2 associated X, apoptosis regulator) and cytosolic cytochrome c

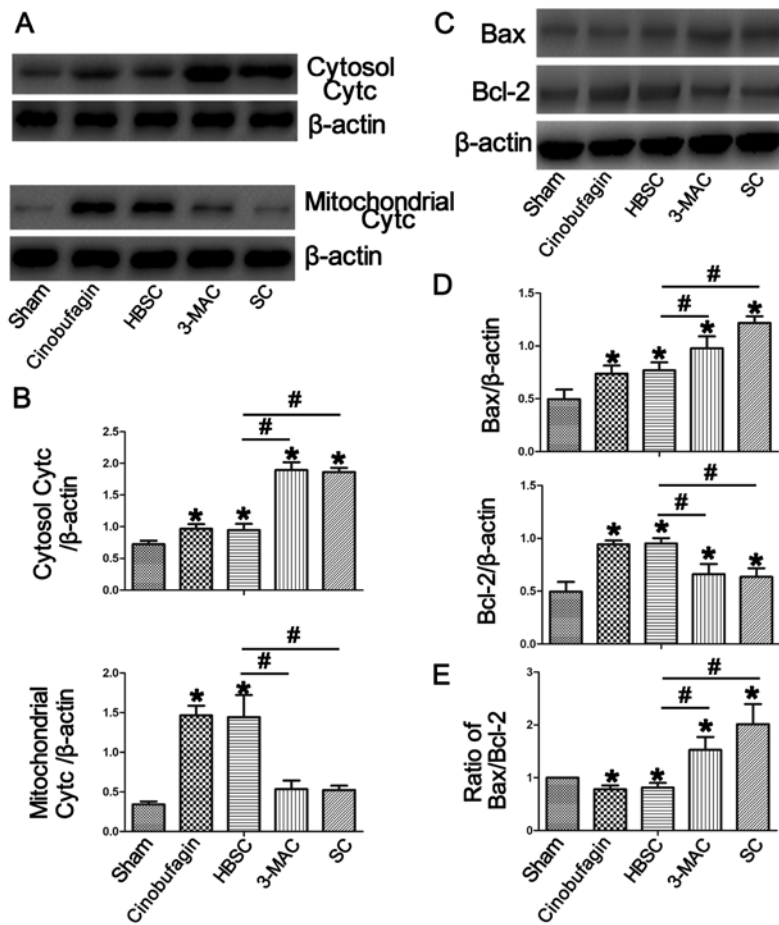


Figure 5. Autophagy inhibition induces Bax and cytochrome *c* expression and reduces Bcl-2. (A and B) After treatment with cinobufagin and downregulation of autophagy in the 3-MAC and SC groups, the expression of cytosolic cytochrome *c* was significantly increased and mitochondrial cytochrome *c* protein was decreased. However, this increase was abrogated in the HBSC group (* $P < 0.05$ compared with the sham group; # $P < 0.05$ compared with the HBSC group). (C and D) Bax was upregulated in the 3-MAC and SC groups compared with the sham and HBSC group, while Bcl-2 was most highly expressed in the HBSC group (* $P < 0.05$ compared with the sham group; # $P < 0.05$ compared with the HBSC group). (E) The ratio of Bax/Bcl-2 was the highest in the 3-MAC and SC groups (* $P < 0.05$ compared with the sham group; # $P < 0.05$ compared with the HBSC group).

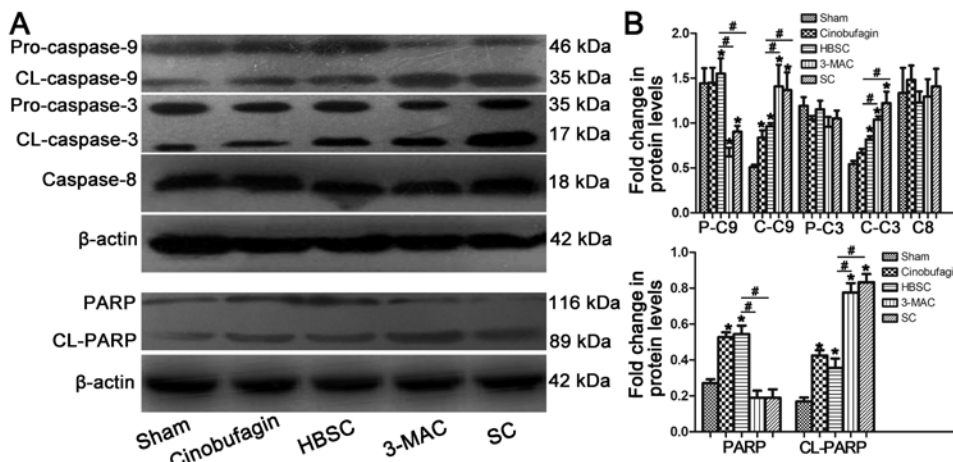


Figure 6. Inhibition of autophagy in SGC-7901 cells induces pro-apoptotic protein expression. (A and B) Pro-apoptotic protein levels were assessed by western blot analysis. Cleaved caspase-3 and cleaved caspase-9 expression was enhanced when autophagy was inhibited in the 3-MAC and SC groups, and this increase was abrogated in the HBSC group. Caspase-8 protein expression was similar between all groups. PARP was analyzed for protein cleavage from the full-length form to the cleaved form by western blot analysis. Inhibition of autophagy promoted PARP protein cleavage (P-C9, Pro-caspase-9; C-C9, CL-caspase-9; P-C3, Pro-caspase-3; C-C3, CL-caspase-3; C8, caspase-8; * $P < 0.05$ compared with the sham group; # $P < 0.05$ compared with the HBSC group).

protein levels compared with the sham group, which was reversed when autophagy was induced in the HBSC

group ($P < 0.05$). In the same way, mitochondrial cytochrome *c* and Bcl-2 (Bcl-2, apoptosis regulator) were upregulated in

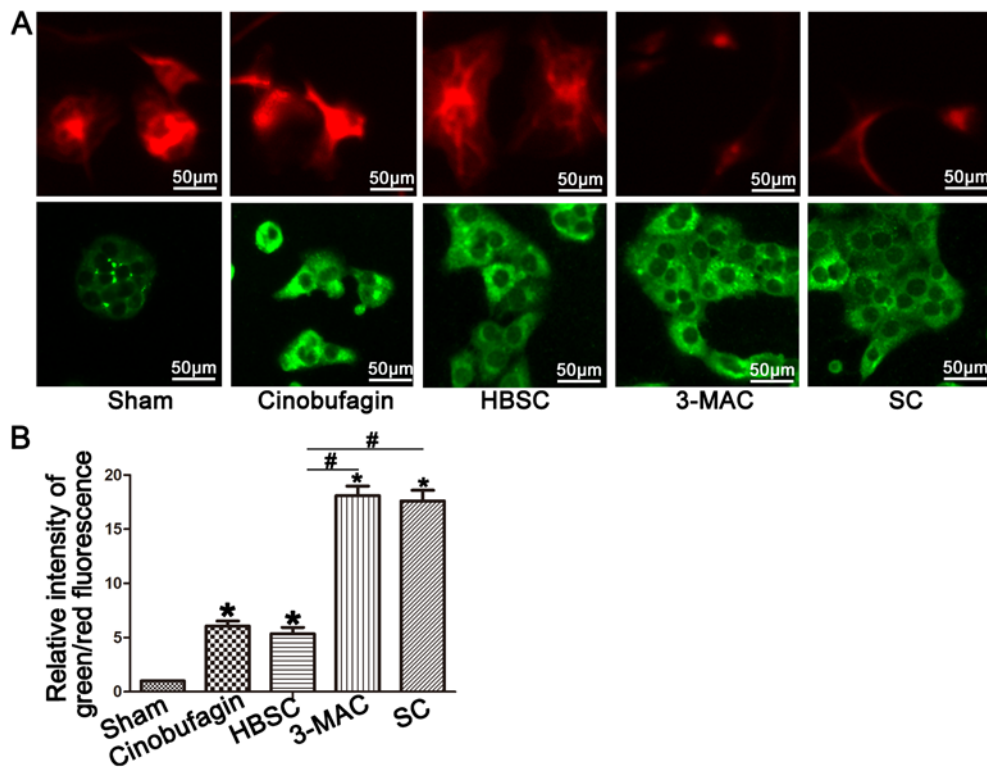


Figure 7. Mitochondrial membrane potential is disrupted in the 3-MAC and SC groups. (A and B) The potential-dependent dye, JC-1, was used to monitor mitochondrial membrane potential. Elevated green fluorescence indicates disrupted mitochondrial membrane potential. Red fluorescence was observed more prominently in the sham and HBSC groups, and green fluorescence was enhanced in the 3-MAC and SC groups (* $P < 0.05$ compared with the sham group; # $P < 0.05$ compared with the HBSC group).

the HBSC group compared with the sham, 3-MAC and SC groups ($P < 0.05$).

Inhibition of autophagy induces pro-apoptotic protein expression. Elevated cleaved caspase-3 and cleaved caspase-9 levels were detected when autophagy was inhibited in SGC-7901 cells; however, this increase was abrogated in the HBSC group. No significant changes in caspase-8 protein expression were observed between any of the groups. Inhibition of autophagy in SGC-7901 cells also promoted the cleavage of PARP [poly(ADP-ribose) polymerase] protein from the full-length form to the cleaved form (Fig. 6; $P < 0.05$).

Mitochondrial membrane potential is disrupted in the 3-MAC and SC groups. Elevated green fluorescence indicates increased mitochondrial membrane potential disruption and mitochondrial depolarization when observed with JC-1. We found increased red fluorescence in the sham and HBSC groups but enhanced green fluorescence in the 3-MAC and SC groups (Fig. 7A and B; $P < 0.05$).

Discussion

In summary, we demonstrated that cinobufagin induced SGC-7901 cell apoptosis, and inhibition of autophagy cooperatively enhanced this effect. These processes may occur partly through ROS generation and activation of the mitochondrial programmed cell death pathway.

Gastric cancer is one of the leading causes of cancer mortality in the world, and is also one of the most common

types of tumors diagnosed in China (1,2). Gastric cancer involves multiple pathways and molecular alterations. As a result, the mechanism and treatment of gastric cancer have been the major focus of cancer research. Due to the high recurrence rates of gastric cancer, it is necessary to identify novel and promising therapeutics.

As medical technology advances, an increasing number of Chinese patent medicines targeting gastric cancer have been filed. Cinobufagin is extracted from Chan Su and was used in Chinese medicine to treat tumors for many years. Cinobufagin has been demonstrated to induce apoptosis in human leukemia, hepatocellular carcinoma and prostate cancer (7,8). Currently, cinobufagin is widely used in the treatment of tumor diseases.

Cinobufagin possesses potent anticancer activity by triggering apoptosis in various types of cancers, including gastric, breast, and hepatic cancer cells. The mechanism of cinobufagin-induced apoptosis involves both the FAS- and mitochondrial-mediated apoptotic pathways (7,18). Additional research has found that cinobufagin induces cytotoxicity in gastric cancer cells by apoptosis, and here we report cell apoptosis of the human gastric cancer cell line SGC-7901 in response to cinobufagin. The basal apoptotic population of the sham group was $2.77 \pm 1.04\%$. After treatment with increasing concentrations of cinobufagin (0.03, 0.06, 0.12 and 0.24 mM) for 24 h, the apoptotic rate increased to 5.99 ± 1.52 , 8.35 ± 2.55 , 12.59 ± 2.25 and $22.91 \pm 4.56\%$, respectively. Thus, we confirmed that cinobufagin increases the apoptosis ratio of gastric cancer cells in a dose-dependent manner.

One study found that inhibition of autophagy by miR-181a overexpression potentiated the toxicity of cisplatin and

reversed drug resistance (13). An increasing number of studies have demonstrated the key role of autophagy in gastric cancer. Autophagy is a process by which cytoplasmic macromolecules or organelles are degraded in lysosomes to maintain cellular homeostasis. Autophagy is an adaptive response to stress and can promote survival; however, it also appears to promote cell death and morbidity (11,19,20). Generally speaking, autophagy is Janus-faced. Some studies have shown that autophagy leads to autophagic cell death under certain conditions, but others have demonstrated that it keeps cells alive under stressful 'life-threatening' conditions. One such study reported that autophagy was activated as a protective mechanism against matrine-induced apoptosis. They found that the inhibition of autophagy enhanced the antitumor potential of matrine in gastric cancer (20). Similarly, we demonstrated that cinobufagin and the inhibition of autophagy, alone or in combination, induced apoptosis in the human gastric cancer cell line SGC-7901.

Apoptosis is a process of programmed cell death that occurs in multicellular organisms and is characterized by blebbing, cell shrinkage, nuclear fragmentation, chromatin condensation, chromosomal DNA fragmentation, and global mRNA decay (21). To the best of our knowledge, apoptosis can be induced by two alternative signaling pathways: The death receptor pathway and the mitochondrial pathway. The action of many anticancer drugs is mediated through the mitochondrial pathway (18,22-24). Additionally, many reports show that cinobufagin is effective in the prevention and treatment of cancer by triggering apoptosis and autophagic cell death via activation of the ROS/JNK/p38 axis (8). Moreover, mitophagy, which is the process of mitochondrial degradation by autophagy, plays a crucial role in cell death and apoptosis (25). Therefore, we focused on the mitochondrial apoptotic pathway when investigating the relationship of cinobufagin, autophagy and apoptosis.

The anti-apoptotic protein Bcl-2 and the pro-apoptotic protein Bax are crucial initiators of the mitochondrial death cascade. Therefore, we first compared Bcl-2 and Bax protein levels in our study. We found decreased expression of Bax and increased expression of Bcl-2 protein when autophagy was induced in the HBSC group. In contrast, downregulation of autophagy by 3-MA or *ATG5* siRNA prevented this enhanced expression. The release of cytochrome *c* from mitochondria into the cytosol is the pivotal factor in the mitochondrial programmed cell death pathway. When autophagy was inhibited, we found that cytosolic cytochrome *c* protein was enhanced and mitochondrial cytochrome *c* protein was accordingly decreased, confirming our initial findings. Caspase-9 is activated after cytochrome *c* is released into the cytosol and undergoes subsequent incorporation into a complex containing cytochrome *c*, apoptotic protease activation factor 1 (APAF1), and procaspase-9. Caspase-9 can activate downstream caspases, including caspase-7 and caspase-3, that eventually lead to apoptosis (26,27). Therefore, we also detected caspase-3 and caspase-9 protein expression. In this study, increased cleaved caspase-3 and cleaved caspase-9 protein expression was observed when autophagy was inhibited in the 3-MAC and SC groups. In contrast, both cleaved caspase-3 and cleaved caspase-9 protein expression was decreased when autophagy was induced in the sham and HBSC groups.

The PARP protein, which plays an important role in the apoptotic pathway, is cleaved by activated caspase-3. Therefore, we compared PARP protein levels between the cell groups in the present study. We found that PARP protein was increasingly cleaved from the full-length 116 kDa form to the cleaved 89 kDa form in the 3-MAC and SC groups. This effect was reversed in the HBSC group. Once the mitochondrial programmed cell death pathway is activated, the mitochondrial permeability transition pore opens and membrane potential decreases (23,24). JC-1 dye is used to monitor mitochondrial membrane potential and exhibits enhanced green fluorescence when membrane potential is disrupted. In this study, we observed more red fluorescence in the sham and HBSC groups, but elevated green fluorescence in the 3-MAC and SC groups. This suggests that mitochondrial membrane potential is disrupted by autophagy inhibition in combination with cinobufagin treatment and could indicate increased cell death.

ROS are chemically reactive oxygen-containing molecules, and examples include peroxides, superoxide, hydroxyl radicals, and singlet oxygen (28). Generation of ROS induced by chemotherapeutic drugs has been observed to trigger the mitochondrial apoptosis pathway (29). Consistent with this observation, we found that cinobufagin induced ROS production in SGC-7901 cells. Inhibition of autophagy further enhanced ROS production and was attenuated by the induction of autophagy. Altogether, these studies suggest that the inhibition of autophagy enhances cinobufagin-induced apoptosis, which may occur, in part, through the mitochondrial programmed cell death pathway.

In summary, we demonstrated that cinobufagin induces SGC-7901 cell apoptosis, which is further enhanced by the inhibition of autophagy. Collectively, this study and previous reports support a model where cinobufagin treatment and autophagy inhibition cooperatively induce SGC-7901 cell apoptosis by enhancing ROS generation and activating the mitochondrial apoptotic pathway. However, the definite relationship between autophagy and mitochondrial apoptotic pathways, and the function of autophagy in the apoptosis pathways, requires further study.

Acknowledgements

Not applicable.

Funding

The present study was supported by grants from the National Science Foundation of China (81670570), Key Research and Development Program of Jiangsu Province (BE2016789) and the Xuzhou City Subject Foundation (KC16SH029).

Availability of data and materials

All data generated or analyzed during this study are included in this published article.

Authors' contributions

YW, XX and TZ designed the research; YW, XX, BL and QZ performed the experiments; YW, XX, MW, HZ, HG and QT

analyzed the data; YW, XX, BL, HG, QT and XL interpreted the results of the experiments; YW, XX, TZ, MW, HZ and QZ prepared the figures; YW, XX, MW, HZ, HG and XL revised the manuscript; YW, XX, BL, QT and TZ approved the final version of the manuscript. All authors read and approved the manuscript and agree to be accountable for all aspects of the research in ensuring that the accuracy or integrity of any part of the work are appropriately investigated and resolved.

Ethics approval and consent to participate

Not applicable.

Patient consent for publication

Not applicable.

Competing interests

The authors state that they have no competing interests.

References

- Jemal A, Bray F, Center MM, Ferlay J, Ward E and Forman D: Global cancer statistics. *CA Cancer J Clin* 61: 69-90, 2011.
- Rugge M, Genta RM, Di Mario F, El-Omar EM, El-Serag HB, Fassan M, Hunt RH, Kuipers EJ, Malfertheiner P, Sugano K, *et al*: Gastric cancer as preventable disease. *Clin Gastroenterol Hepatol* 15: 1833-1843, 2017.
- Greenlee RT, Hill-Harmon MB, Murray T and Thun M: Cancer statistics, 2001. *CA Cancer J Clin* 51: 15-36, 2001.
- Brenner H, Rothenbacher D and Arndt V: Epidemiology of stomach cancer. *Methods Mol Biol* 472: 467-477, 2009.
- Lim SC, Parajuli KR, Duong HQ, Choi JE and Han SI: Cholesterol induces autophagic and apoptotic death in gastric carcinoma cells. *Int J Oncol* 44: 805-811, 2014.
- Zhang Y, Tang X, Liu X, Li F and Lin X: Simultaneous determination of three bufadienolides in rat plasma after intravenous administration of bufadienolides extract by ultra performance liquid chromatography electrospray ionization tandem mass spectrometry. *Anal Chim Acta* 610: 224-231, 2008.
- Mommersteeg MC, Yu J, Peppelenbosch MP and Fuhler GM: Genetic host factors in *helicobacter pylori*-induced carcinogenesis: Emerging new paradigms. *Biochim Biophys Acta* 1869: 42-52, 2018.
- Ma K, Zhang C, Huang MY, Li WY and Hu GQ: Cinobufagin induces autophagy-mediated cell death in human osteosarcoma U2OS cells through the ROS/JNK/p38 signaling pathway. *Oncol Rep* 36: 90-98, 2016.
- Rautou PE, Mansouri A, Lebrech D, Durand F, Valla D and Moreau R: Autophagy in liver diseases. *J Hepatol* 53: 1123-1134, 2010.
- Nivon M, Richet E, Codogno P, Arrigo AP and Kretz-Remy C: Autophagy activation by NF κ B is essential for cell survival after heat shock. *Autophagy* 5: 766-783, 2009.
- Mizushima N, Levine B, Cuervo AM and Klionsky DJ: Autophagy fights disease through cellular self-digestion. *Nature* 451: 1069-1075, 2008.
- Kumar A, Singh UK and Chaudhary A: Targeting autophagy to overcome drug resistance in cancer therapy. *Future Med Chem* 7: 1535-1542, 2015.
- Zhao J, Nie Y, Wang H and Lin Y: MiR-181a suppresses autophagy and sensitizes gastric cancer cells to cisplatin. *Gene* 576: 828-833, 2016.
- Xiong X, Wu M, Zhang H, Li J, Lu B, Guo Y, Zhou T, Guo H, Peng R, Li X, *et al*: *Atg5* siRNA inhibits autophagy and enhances norcantharidin-induced apoptosis in hepatocellular carcinoma. *Int J Oncol* 47: 1321-1328, 2015.
- Settembre C, Di Malta C, Polito VA, Garcia Arencibia M, Vetrini F, Erdin S, Erdin SU, Huynh T, Medina D, Colella P, *et al*: TFEB links autophagy to lysosomal biogenesis. *Science* 332: 1429-1433, 2011.
- Carchman EH, Rao J, Loughran PA, Rosengart MR and Zuckerbraun BS: Heme oxygenase-1-mediated autophagy protects against hepatocyte cell death and hepatic injury from infection/sepsis in mice. *Hepatology* 53: 2053-2062, 2011.
- Lewis JS, Meeke K, Osipo C, Ross EA, Kidawi N, Li T, Bell E, Chandel NS and Jordan VC: Intrinsic mechanism of estradiol-induced apoptosis in breast cancer cells resistant to estrogen deprivation. *J Natl Cancer Inst* 97: 1746-1759, 2005.
- Qi F, Inagaki Y, Gao B, Cui X, Xu H, Kokudo N, Li A and Tang W: Bufalin and cinobufagin induce apoptosis of human hepatocellular carcinoma cells via Fas- and mitochondria-mediated pathways. *Cancer Sci* 102: 951-958, 2011.
- Reed M, Morris SH, Jang S, Mukherjee S, Yue Z and Lukacs NW: Autophagy-inducing protein beclin-1 in dendritic cells regulates CD4 T cell responses and disease severity during respiratory syncytial virus infection. *J Immunol* 191: 2526-2537, 2013.
- Chen YY, Sun LQ, Wang BA, Zou XM, Mu YM and Lu JM: Palmitate induces autophagy in pancreatic β -cells via endoplasmic reticulum stress and its downstream JNK pathway. *Int J Mol Med* 32: 1401-1406, 2013.
- Xie SQ, Zhang YH, Li Q, Xu FH, Miao JW, Zhao J and Wang CJ: 3-Nitro-naphthalimide and nitrogen mustard conjugate NNM-25 induces hepatocellular carcinoma apoptosis via PARP-1/p53 pathway. *Apoptosis* 17: 725-734, 2012.
- Shen B, He PJ and Shao CL: Norcantharidin induced DU145 cell apoptosis through ROS-mediated mitochondrial dysfunction and energy depletion. *PLoS One* 8: e84610, 2013.
- Zhang JY, Lin MT, Tung HY, Tang SL, Yi T, Zhang YZ, Tang YN, Zhao ZZ and Chen HB: Bruceine D induces apoptosis in human chronic myeloid leukemia K562 cells via mitochondrial pathway. *Am J Cancer Res* 6: 819-826, 2016.
- Lin M, Tang S, Zhang C, Chen H, Huang W, Liu Y and Zhang J: Euphorbia factor L2 induces apoptosis in A549 cells through the mitochondrial pathway. *Acta Pharm Sin B* 7: 59-64, 2017.
- Kim I and Lemasters JJ: Mitophagy selectively degrades individual damaged mitochondria after photoirradiation. *Antioxid Redox Signal* 14: 1919-1928, 2011.
- Zhang JY, Yi T, Liu J, Zhao ZZ and Chen HB: Quercetin induces apoptosis via the mitochondrial pathway in KB and KBv200 cells. *J Agric Food Chem* 61: 2188-2195, 2013.
- Wang XH, Jia DZ, Liang YJ, Yan SL, Ding Y, Chen LM, Shi Z, Zeng MS, Liu GF and Fu LW: Lgf-YL-9 induces apoptosis in human epidermoid carcinoma KB cells and multidrug resistant KBv200 cells via reactive oxygen species-independent mitochondrial pathway. *Cancer Lett* 249: 256-270, 2007.
- Kang JY, Eggert M, Mouli S, Aljuffali I, Fu X, Nie B, Sheil A, Waddey K, Oldham CD, May SW, *et al*: Pharmacokinetics, antitumor and cardioprotective effects of liposome-encapsulated phenylaminoethyl selenide in human prostate cancer rodent models. *Pharm Res* 32: 852-862, 2015.
- Ott M, Gogvadze V, Orrenius S and Zhivotovsky B: Mitochondria, oxidative stress and cell death. *Apoptosis* 12: 913-922, 2007.